



Molecular Crystals and Liquid Crystals

Publication details, including instructions for authors and subscription information:

<http://www.tandfonline.com/loi/gmcl16>

The effect of Carbonyl Containing Substituents in the Terminal chains on Mesomorphic Properties in Aromatic Esters and Thioesters, 2. Acyloxy Groups on the Phenolic End

Mary E. Neubert^a, Patricia J. Wildman^{a b}, Michael J. Zawaski^{a c}, Carol A. Hanlon^a, Theresa L. Benyo^a & Adriaan De Vries^a

^a Liquied Crystal Institute, Kent State University, Kent, Ohio, 44242

^b Thibodaux, Louisiana

^c Aurora, Ohio

Version of record first published: 19 Dec 2006.

To cite this article: Mary E. Neubert, Patricia J. Wildman, Michael J. Zawaski, Carol A. Hanlon, Theresa L. Benyo & Adriaan De Vries (1987): The effect of Carbonyl Containing Substituents in the Terminal chains on Mesomorphic Properties in Aromatic Esters and Thioesters, 2. Acyloxy Groups on the Phenolic End, *Molecular Crystals and Liquid Crystals*, 145:1, 111-157

To link to this article: <http://dx.doi.org/10.1080/00268948708080217>

PLEASE SCROLL DOWN FOR ARTICLE

Full terms and conditions of use: <http://www.tandfonline.com/page/terms-and-conditions>

This article may be used for research, teaching, and private study purposes. Any substantial or systematic reproduction, redistribution, reselling, loan, sub-licensing, systematic supply, or distribution in any form to anyone is expressly forbidden.

The publisher does not give any warranty express or implied or make any representation that the contents will be complete or accurate or up to date. The accuracy of any instructions, formulae, and drug doses should be independently verified with primary sources. The publisher shall not be liable for any loss, actions, claims, proceedings, demand, or costs or damages whatsoever or howsoever caused arising directly or indirectly in connection with or arising out of the use of this material.

Mol. Cryst. Liq. Cryst., 1987, Vol. 145, pp. 111–157

Photocopying permitted by license only

© 1987 Gordon and Breach Science Publishers S.A.

Printed in the United States of America

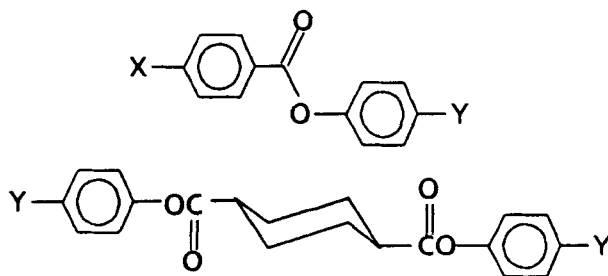
The Effect of Carbonyl Containing Substituents in the Terminal Chains on Mesomorphic Properties in Aromatic Esters and Thioesters, 2. Acyloxy Groups on the Phenolic End

MARY E. NEUBERT, PATRICIA J. WILDMAN,[†] MICHAEL J. ZAWASKI,[‡] CAROL A. HANLON, THERESA L. BENYO and ADRIAAN DE VRIES

Liquid Crystal Institute, Kent State University, Kent, Ohio 44242

(Received October 28, 1986)

The effect of replacing an alkoxy ($Y=OR'$) with an acyloxy ($Y=OCOR'$) group on the phenolic end of the esters:



on their mesomorphic properties has been studied. These esters were prepared by esterification of 4-acyloxyphenols with the appropriate acid chloride. The phenols were synthesized by acylation of 4-benzyloxyphenol with either an aliphatic acid or acid chloride followed by catalytic hydrogenolysis of the benzyl group.

A comparison of the melting and clearing temperatures of these acyloxy esters with the corresponding known alkoxy ones showed small increases in both these temper-

[†]Current address: Thibodaux, Louisiana.

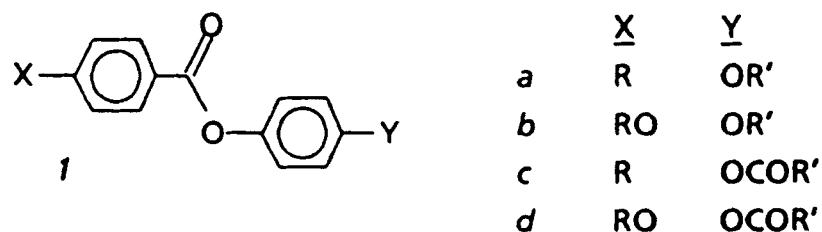
[‡]Current address: Aurora, Ohio.

atures for the acyloxy esters. The same types of mesophases (N , S_A , S_C , S_B) were observed in both series, but the S_B was more favored when $Y=OCOR'$. The S_C phase was found to occur in the acyloxy series at chain lengths beyond which it disappeared in the alkoxy series.

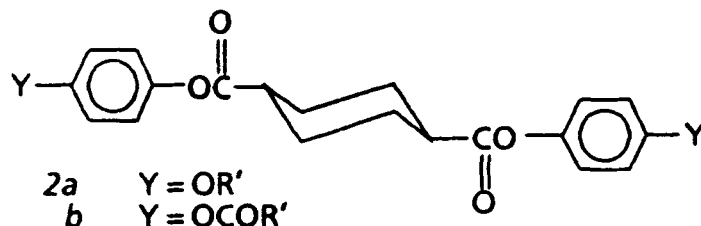
Comparisons were also made with the mesomorphic properties previously reported for the corresponding alkyl and α -keto esters. Some correlation was observed between increasing dipole moments of these substituents and increasing transition temperatures but not in the types of mesophases observed. Fewer mesophases were found when the alkyl chain was attached to the benzene ring through a carbon atom than through an oxygen atom.

INTRODUCTION

As part of our interest in studying the effect of a carbonyl containing group in the terminal substituents on the mesomorphic properties of aromatic esters,¹ the 4-acyloxybenzoates *1c* and *d*

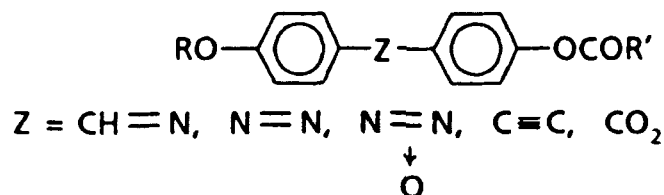


and the corresponding cyclohexane diesters *2b*:



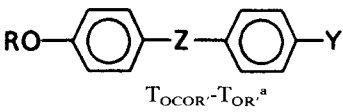
were prepared and their mesomorphic properties determined.

Mesomorphic properties for a variety of compounds with the general structure:



have been reported. A comparison of the melting transition for the OCOR' with the OR' series (Table I) shows that for all the central groups except the esters, this temperature is lower in the OCOR' series. For the anils, azo, and azoxy compounds this decrease is fairly large, 12–47°. In general, the clearing transitions are also lower but not as consistently and by a smaller amount. The esters, however, generally show an increase in both the melting and clearing temperatures, although not by a large amount. Since the chain lengths of the homologs reported that could be compared are short to mid-chain

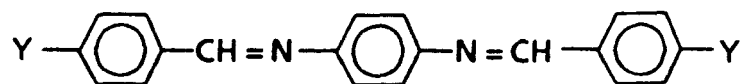
TABLE I
Comparison of Mesomorphic Properties for

<div style="text-align: center;">  </div>					
Z	R	Total carbons in Y	melting	clearing	N Phase Range for OCOR' -OR'
CH=N	C ₅	2	-15	-14	1.0
		3	-22	3.5	26
		4	-38.5	-11	~26 ^b
		5	-31.5	-3.5	~22 ^b
N=N	C ₃	3	-47.1	7	~20 ^b
		4	-37	0	~26 ^b
		5	-27	-4	~18 ^b
		6	-20	-3	17
		7	-24	-8	-1
N=N ↓ O	C ₂	2	-38.6	-16.5	22
		C ₃	-26.5	-5.6	21
		C ₄	-23	-1.7	21
		C ₅	-17.5	-6.2	11
C≡C	C ₆	6	-15.3	-7.1	8
		7	-12.4	-6.2	0
		C ₁	-3.5	2	~5 ^c
		6	-3.5	-8	-7
CO ₂	C ₆	2	10	-0.9	-11
		3	4	14.7	11
		4	0	10	10
		5	-3	6.5	9
		6	9.5	6	-3
		7	9	6	-3
		8	9	6	-3
		9	5.5	4.8	0

^aT = transition temperature in degrees centigrade; calculated using data from Ref. 2.

length, few smectic properties were observed; most of these compounds have only N^\dagger phases. The N phase length generally increases in the OCOR' series for the anils, azo, and azoxy compounds but fluctuates for the alkynes and esters between being larger or smaller.

The only series of compounds with a terminal acyloxy group with a structure similar to that of the cyclohexane diesters **2** that has been reported is the phenylenediamine series:²



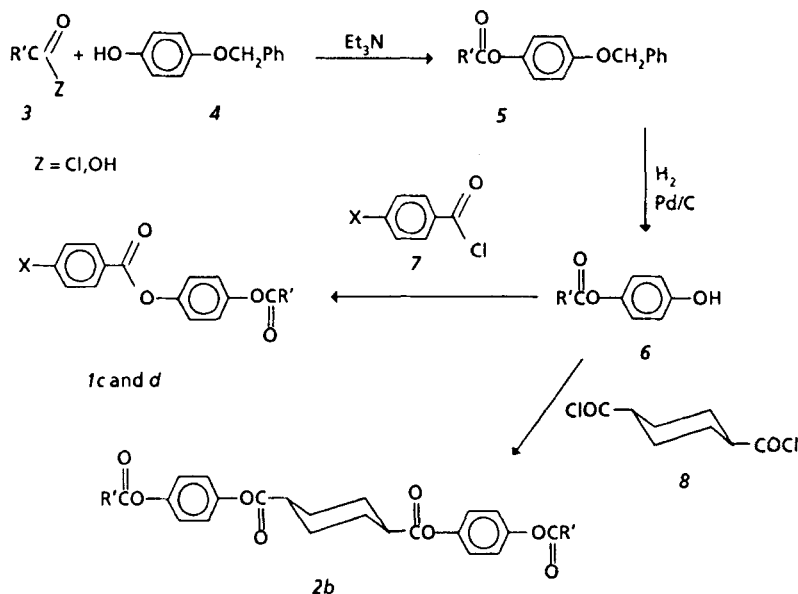
In this series, the melting temperatures were 19–20° lower in the OCOR' than in the OR' series and the clearing temperatures were ~2–26° higher. Both N and S phases were observed in these two series. The N phase range increased only slightly in the OCOR' series but the total S phase range increased substantially, especially at carbon chain lengths greater than C_4 (35–115°).

Although the mesomorphic properties of some of the acyloxybenzoates **1d** have been reported and the effect of this structural change on the N phase can be determined, longer chain homologs are needed to study the effect on smectic phases. None of the acyloxycyclohexane diesters **2b** or the analogous terephthalic acid diesters have been studied. Additionally, both the phenylbenzoates **1c** and **d** and the cyclohexane diesters **2b** are needed as standards for comparison with compounds that will be studied later with the acyloxy group moved further along the chain away from the benzene ring.

SYNTHESIS

The acyloxyphenylbenzoates **1c** and **d** and the corresponding cyclohexane diesters **2b** were prepared by esterification of the acyloxyphenol **6** with the appropriate acid chlorides **7** and **8** (Scheme 1) using triethylamine as the base.³ Purified yields of the phenylbenzoates ranged from 26–94%. Finding a good recrystallizing solvent for many of these esters was difficult. Some tended to form gels instead of crystals, particularly when $X=R$. When $X=RO$, absolute ethanol worked best for $R'=C_1-C_9$. The longer and less soluble homologs required the addition of some chloroform to the ethanol. This mixture

[†]See the experimental section for definitions of abbreviations.



SCHEME 1

was also used to recrystallize the esters with $X=R$. Attempts to prepare these esters using the carbodiimide method with methylene chloride as the solvent⁴ gave low yields when $R'=C_1$ and C_2 and $X=C_{10}O$. These homologs also had to be chromatographed (silica gel) and then recrystallized from ligroine to obtain pure materials. Determination of transition temperatures for these esters before and after chromatography indicated that the trace impurity shown to be present by thin-layer chromatography (TLC) had a negligible effect on the transition temperatures.

Purified yields of the cyclohexane diesters **2b** ranged from 11–83%. These compounds were even more difficult to purify than the phenylbenzoates which is the reason for many of the low yields. Solubilities varied throughout this series with the short and long homologs being less soluble than the mid-chain length ones. These esters were recrystallized from a mixture of absolute ethanol with either chloroform or methylene chloride; more details are provided in the experimental section. Again the C_2 and C_3 homologs were purified by column chromatography.

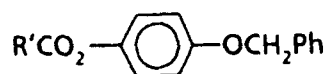
The acyloxyphenols **5** with $R'=C_1$ – C_{17} were prepared by acylating 4-benzyloxyphenol (**4**) with an acid chloride **3** ($Z=Cl$) using the same method as employed to prepare the esters **1c** and **d** and **2b**. When

$R'=C_{21}$, the acid chloride was not commercially available so the acid was used in a carbodiimide esterification. Examples of these methods are given in the experimental section. Debenzylation of these esters 5 by hydrogenation over Pd-C gave the acyloxyphenols 6. Data for the benzyl ethers are presented in Table II and for the phenols in Table III. The phenols 6 were recrystallized from either ligroine or a combination of ligroine and ethyl acetate depending on their solubilities. The phenol with $R=C_{21}$ was too insoluble to be recrystallized and was therefore used without purification.

The catalytic hydrogenolysis was initially done using 10% Pd/C in ethanol at ca. 50 psi until no further drop in hydrogen pressure was observed. Since it was necessary to heat the reaction mixture to obtain a solution, the reaction temperature initially used was 72°. However, when the C_8 homolog was hydrogenated at this temperature for 48 hours, TLC of the isolated material showed not only a spot for the

TABLE II

Data for



R'	Purified Yield (%) ^a	mp (°C)	Recrystallizing Solvent ^b
C ₁	53.0	116–118	L
C ₂	69.0	92–93	L
C ₃	93.7	79–82	E
C ₄	54.8	62–64	E
C ₅	84.3	63–65	E
C ₆	78.2	63–66	L
C ₇	83.8	65.0–65.5	L
C ₈	64.6	72–74	L
C ₉	80.8	75–77	L
C ₁₁	95.2 ^c	80–81.5	L
C ₁₃	91.1 ^c	79–85	E
C ₁₅	94.0 ^c	87–90	E
C ₁₇	73.2	88–90	L
C ₂₁	18.0 ^d	95–96	L

^aYield after 3 recrystallizations unless otherwise noted.

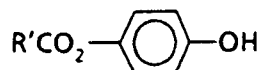
^bL = ligroine, E = absolute EtOH.

^cYield after 1 recrystallization.

^dPrepared using DCC in CH₂Cl₂.

TABLE III

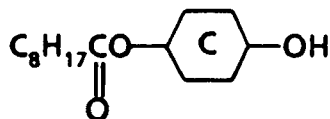
Data for



R'	Purified Yield (%) ^a	mp (°C)
C ₁	45.3	62–63
C ₂	83.3	78–80
C ₃	64.4	53–55
C ₄	90.2	50–52
C ₅	85.2	59–60
C ₆	75.0	55–58
C ₇	70.2	72–74.5
C ₈	43.0	71–74
C ₉	64.4	79–83
C ₁₁	78.4	88–90
C ₁₃	41.6	90–92.5
C ₁₅	68.9	95–98
C ₁₇	29.6	95–97
C ₂₁	42.9 ^b	102–103

^aYield after 2–3 recrystallizations unless otherwise noted.^bNot recrystallized.

desired phenol 6 but also one with an R_f value similar to that observed for the starting benzyl ether 5. Thinking that this reduction was incomplete, it was repeated at 72° for another 5 hours with fresh catalyst. The material isolated this time showed only one spot by TLC with an R_f value near that of the starting benzyl ether. An NMR spectrum of this material showed no aromatic or α -aromatic methylene protons and the addition of a complex multiplet at ~ 2.6 – 2.0δ . Distillation of this liquid gave a material which IR, NMR, and elemental analysis confirmed was the cyclohexane alcohol:



NMR also indicated that distillation had given predominately the *trans* isomer. This ring reduction is being studied more extensively to try

to determine the best conditions for obtaining total ring reduction and isolating the *trans* isomer so that these alcohols can be used to prepare other new mesogens. More details will be presented in a later paper.

To avoid reduction of the aromatic ring, several variations in the reaction conditions were tried. The benzyl ether was dissolved in ethanol at 50–80°, hydrogenated at this temperature for 15 min until enough of the phenol formed to maintain a solution without heating,[†] and then the heat removed while the reduction was continued for another 1–3 hr. None of the cyclohexane alcohol was detected in material isolated using these conditions. Similar variations such as shorter reaction times with heating throughout the reduction were equally successful. Eventually, it was found that reduction at ~50° for 1–2 hr using 5% Pd/C was sufficient to cleave the benzyl ether and this became the preferred method.

Typical detailed procedures used to prepare these compounds are given in the experimental section. NMR data used to identify these structures are presented in Table IV. Proton identifications were made with the help of data previously reported for the alkyl and alkoxy esters *1a* and *b*.⁵

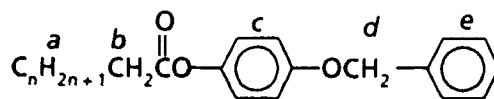
MESOMORPHIC PROPERTIES

Transition temperatures for the acyloxyphenylbenzoates *1c* and *d* prepared are presented in Table V. Although we now know that it is not necessary to synthesize a homologous series to determine the trends in mesomorphic properties in a particular structure, this was not so obvious at the time these esters were prepared. Additionally, the problems observed with identifying the *S_B* phase near the melting temperature (discussed in more detail under microscopic studies) and the discovery that more smectic phases were observed at longer chain lengths than is usually found made it necessary to prepare more homologs than was initially planned.

A comparison of the mesomorphic properties of the alkyl series where $X=C_{10}$ and $Y=OCOR'$ with those reported for the corresponding $Y=OR'$ series in which the total number of carbon atoms

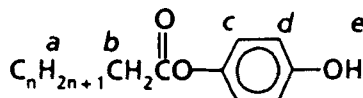
[†]The ether will not reduce if it crystallizes from the solution during hydrogenation.

TABLE IV
NMR Data for



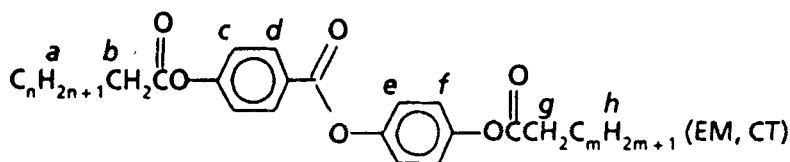
$n = 1$: 1.82.25 (s, CH₃ in *a*)-EM, CD
 $n = 2$: 2.82.56 (*q*, *b*) and 1.25 (t, CH₃ in *a*) with $J = 7.0$ Hz-FT, CD
 $n = 3$: 3.82.39 (*t*, *b*), 1.69 (sext., CH₂ in *a*) and 0.99 (t, CH₃ in *a*) with $J = 7.0$ Hz-EM, CT
 $n > 3$: 9EM, CT):

δ	# of Protons	Multiplicity	J (Hz)	ID
7.37	5	s	—	<i>e</i>
6.96	4	s	—	<i>c</i>
5.02	2	s	—	<i>d</i>
2.52	2	t	7.0	<i>b</i>
1.30–0.88	$2n + 1$	m	—	<i>a</i>



$n = 1$: 1.82.27 (s, CH₃ in *a*)-FT, CD
 $n = 2$: 2.82.52 (*q*, *b*) and 1.43 (t, CH₃ in *a*) with $J = 7.0$ Hz-FT, CD
 $n = 3$: 3.82.50 (*t*, *b*), 1.78 (sext., CH₂ in *a*) and 1.0 (t, CH₃ in *a*) with $J = 7.0$ Hz
 $n > 3$:

6.87	2	d	9.0	<i>c</i>
6.45	2	d	9.0	<i>d</i>
5.79	1	s	—	<i>e</i>
2.46	2	t	7.0	<i>b</i>
2.0–1.7	$2n + 1$	m	—	<i>a</i>

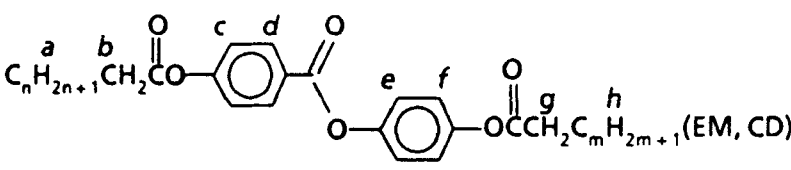
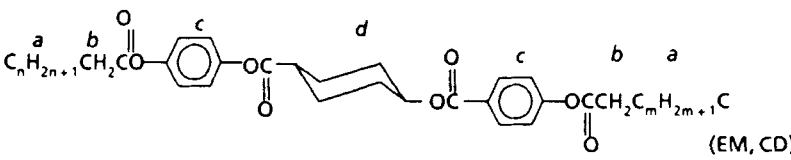


8.07	2	d	9.0	<i>d</i>
7.26	2	c	9.0	<i>d</i>
7.13	4	s	—	<i>e + f</i>
2.68	2	t*	7.0	<i>g</i>
2.49	2	t*	7.0	<i>b</i>
2.0–1.7	$2n + 1, 2m + 1$	m	—	<i>a + h</i>

(continued)

TABLE IV (cont.)

NMR Data for

δ	# of Protons	Multiplicity	J (Hz)	ID
				
8.17	2	d	9.0	d
7.18	4	s	—	e, f
6.93	2	d	9.0	c
4.02	2	t	6.0	b
2.58	2	t	7.0	g
2.0–1.7	2n + 1.2m + 1	m	—	a + h
				
$n = 2: \delta 2.6$ (q, b) and 1.23 (t, CH ₃ in a) with $J = 7.0$ Hz $n > 3$:				
7.11	8	s	—	c
2.51	2	t	7.0	b
2.4–0.8	2(2n + 1)	m	—	a

m = unresolved multiplet, q = quartet, s = singlet and t = triplet.

*overlapping triplets which are not well resolved.

in Y is used† is made in Figure 1 (see also Table VI). Both the melting and clearing temperatures increase with increasing chain length and are higher for the OCOR' series. In all three homologs, the melting temperatures increase more than the clearing ones with this increase

†It is difficult to decide whether to compare the total number of carbon atoms in chains containing carbonyl groups or only the number of carbons in the alkyl chain R'. The former considers the carbonyl group as part of the chain; the latter as part of the rigid core. Both comparisons were made but little difference could be seen in the trends observed in the two series. More regular alternations of the data could sometimes be seen when R's were compared. The plots in Figures 2 and 3 make it possible to compare either set of data for these esters.

decreasing with increasing chain length for the melting transition but remaining fairly constant for the clearing one. Replacement of the OR' with the OCOR' group seems less favorable for all the mesophases observed. The *N* phase predominates but is primarily monotropic. The only *S* phase observed, a monotropic *S_C* phase, occurred in the *C₈* homolog. Since this series showed so few mesophases, no additional homologs were prepared.

The alkoxy series *Id* proved to be more interesting (Table V). A comparison of the plots of the transition temperatures versus the total number of carbon atoms in Y for Y=OR' and Y=OCOR' and for

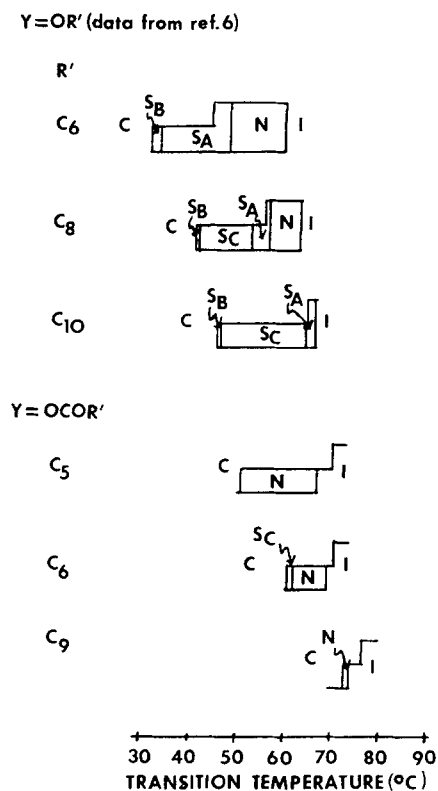


FIGURE 1 Comparison of Mesomorphic Properties for

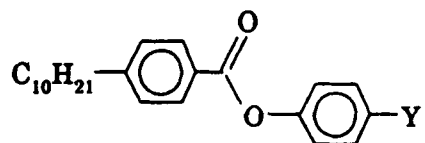
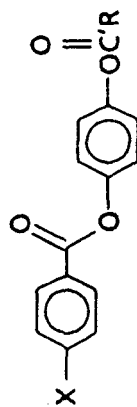


TABLE V
Transition Temperatures (°C) for



X	R'	C	S _B	S _C	S _A	N	I ^a
C ₁₀	C ₅	50.5				(66.4–66.7)	68.5–68.9
	C ₇	60.7		(61.4–61.7)	—	68.7–69.0	70.1–70.4
	C ₉	72.6		—	—	(72.7)	76.5–76.9
C ₆ O	C ₄	55.3		(60.5–62.2)	—	65.9–66.5	94.2–94.3 ^b
	C ₂	52.2		64.6	—	65.8–66.3	93.7–94.3
C ₈ O	C ₉	46.6		65.1–67.3	—	80.7–81.0	95.7–95.8
C ₁₀ O	C ₁	54.5		—	(60.3)	68.4–70.8	89.4–89.6 ^b
	C ₂	57.0	67.8–69.8	—	—	70.4–70.5	94.1–94.2 ^b
	C ₅	54.0	~65.3	—	71.1–71.9	72.9–73.0	97.2–97.5 ^b

C ₄	52.0	65.2–65.6	—	68.2–68.3	73.4–73.5	93.7–94.1
C ₅	RT ^c	67.7–68.9	71.4–72.2	—	75.3–75.4	93.6–94.0
C ₆	0	(68.7)	69.8–70.0	—	80.5	92.3
C ₇	36	(63.8–64.1)	73.0–73.6	—	85.0	94.8–94.9
C ₈	39	(62.5–63.6)	68.8–69.3	—	87.3–87.6	94.8–95.1
C ₉	48.2	(60.3–61.6)	68.7–69.4	—	90.4–91.5	96.0–96.8
C ₁₁	57.6	—	68.5–69.7	—	93.1–93.5	94.8–95.3
C ₁₃	67.4	—	73.8–74.5	—	—	95.0–95.8
C ₁₅	71.9	—	78.0–79.3	—	—	94.7–95.1
C ₁₇	76.6	—	82.5–83.1	—	—	93.9–94.4
C ₂₁	87.7	—	89.5–89.9	—	—	91.4–91.7
C ₁₂ O	~62.5 ^d	61.2–61.9	66.0–66.8	70.6–70.9	82.4–82.7	93.3–94.4
C ₉	~46.0 ^d	~ 69.6–72.1	74.0–74.3	—	95.8–97.1	97.7

() Indicates a monotropic transition.

^aDefinitions for these letters are given in the experimental section.

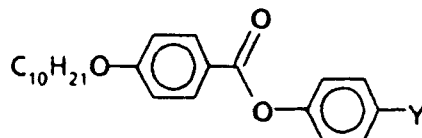
^bTransition temperatures previously reported in Ref. 2: X=C₆O, R'=C₄, 68 (N), 93 (I); X=C₁₀O, R'=C₁, 87 (S_A), 99.6 (I), R'=C₂, 87 (S_A) 130.5 (I), R'=C₃, 98.5 (S_A), 116 (I), and R'=C₄, 95 (S_A), 123° (I).

^cCrystallization was slow so the sample was allowed to set overnight to crystallize.

^dEstimated from DSC scans.

^eOverlapping transitions.

TABLE VI
Comparison of Transition Temperatures (°C) for



Total Carbons in Y	Differences in Temperatures ^a	
	mp	clp
6	24.8	7.7
8	13.8	7.9
10	12.4	8.1

^aTransition temperature for Y=OCOR' minus that for Y=OR'.

X=C₁₀O is presented in Figure 2.† A stronger odd-even alternation in the clearing temperatures occurs when Y=OR' than with Y=OCOR'. In both series, this curve levels off at longer chain lengths and the curve for chain lengths >12C‡ in the OCOR' series falls gradually at longer chain lengths. In both series, the maximum clearing temperature occurs in the short homologs; at 2C and 92.3° when Y=OR' and at 4C and 97.5° when Y=OCOR'. The minimum in the melting curves occurs at about the same chain length at 3C and 60.5° when Y=OR' and at 4C (the same homolog which has the maximum clearing temperature) and 65.3° when Y=OCOR'. This curve rises much more slowly when Y=OCOR' and does not show the odd-even alternation observed when Y=OR'. At 22C, it appears that the melting curve will soon intersect with the falling clearing curve with loss of mesomorphic properties probably at 23C whereas this will occur at ca. 16C in the OR' series.

A comparison of the differences in melting temperatures for each homolog of these two series (Table VII) shows that these can be either higher or lower in the OCOR' series than in the OR' series

†Data for the Y=OR' series was taken from references 2 and 5. Transition temperatures for R'=C₁₀ were incorrectly reported in Reference 5. The correct temperatures are: 70.1–71.5° (C→S_c), 87.3–87.6° (S_c→S_A), 88.9–89.1° (S_c→N), 90.2–90.5° (N→I), and 60.7° (S_c→C). The R'=C₁₄ homolog is a new compound. Transition temperatures are given in the experimental section.

‡This abbreviation is used to indicate the total number of carbon atoms in a terminal substituent as compared to C_n for the alkyl (R') chain length.

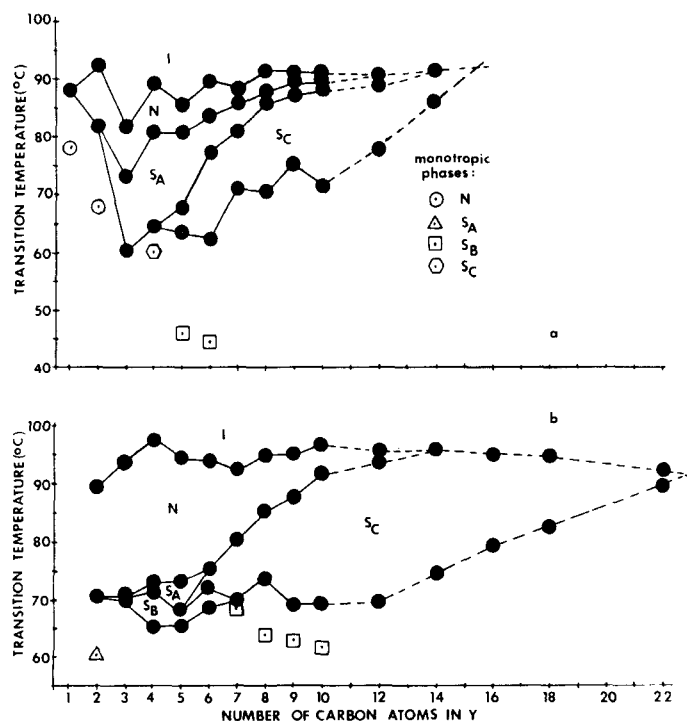
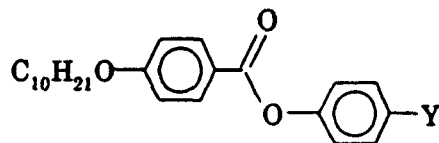


FIGURE 2 Transition Temperatures ($^{\circ}\text{C}$) Versus the Number of Carbon Atoms in Y for

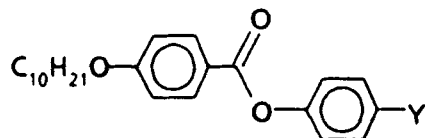


- a. $\text{Y}=\text{OR}'$ (data from references 2 and 5).
b. $\text{Y}=\text{OCOR}'$

by a range of -11.2 to $+9.3^{\circ}$ although an increase occurs more often than a decrease. Clearing temperatures were always higher in the OCOR' series (except for the 2C homolog) with the difference varying from 3.4 – 12° .

The same types of mesophases were observed in both the OR' and OCOR' series (Table VII). However, as was true when $\text{X}=\text{R}$, the nematic phase seems to be more favored when $\text{Y}=\text{OCOR}'$ having a wider range and persisting at a slightly longer chain length. Replacement of the OR' chain by the OCOR' group does not seem to favor formation of the S_A phase which disappears at 6C when

TABLE VII
Comparison of Mesomorphic Properties for



Total No. Carbons in Y	$\Delta(T_{\text{OCOR}} - T_{\text{OR}})^{\circ}\text{C}$	
	melting	clearing
2	-10.9	-2.7
3	9.3	12
4	0.8	8.4
5	2.1	8.6
6	6.4	4.5
7	-1.0	3.8
8	3.1	3.4
9	5.7	4.1
10	-2.1	6.3
12	-7.8	4.8
14	-11.2	6.7

Total Carbons for		
Mesophase Change	OR'	OCOR'
N lost	~12	14
S _A lost	14	6
S _C enters	4	6
S _B occurs	5, 6	3-10

$\text{Y}=\text{OCOR}'$ as compared to its presence until 14C when $\text{Y}=\text{OR}'$. This change also causes the S_C phase to enter the OCOR' series at a chain length 2 carbons longer at 6C than when $\text{Y}=\text{OR}'$. Surprisingly, this phase is still present at 22C and has a much wider range at long chain lengths with a maximum at 24.6° at 12C. The predicted intersection point for the OR' series mentioned earlier suggests that the S_C phase will be lost by 16C in this series. The OCOR' group also seems to favor formation of the S_B phase which occurred in more homologs than when $\text{Y}=\text{OR}'$. Even so, this phase was often monotropic and always had a short phase range.

Our data for the esters *Id* with $X=C_{10}O$ and $R'=C_1-C_4$ do not agree with that reported in the literature (see Table V).² Transition temperatures were carefully rechecked and NMR data obtained for both the intermediates and the esters to convince us that the structural assignments are correct. Since the primary source of the literature data has not yet been published, we are unable to comment on why these data are so different.

Although the esters *Id* with $X=C_{10}O$ showed smectic polymorphism, shorter homologs did not, as shown by the data for $X=C_6O$ and C_8O (Table V) which has only *N* and *S_C* phases. However, the polymorphism observed in the $C_{10}O$ series continued in the $C_{12}O$ series. This emphasizes the need to prepare long chain homologs (i.e. $>C_8O$) before making conclusions about smectic trends in a series.

The effect of replacing the OR' group with an acyloxy group in the cyclohexane diesters *2b* is presented in plots of transition temperatures *versus* the total number of carbon atoms in *Y* in Figure 3 and the data in Table VIII. From Figure 3, it is obvious that this structural modification causes the melting temperatures to increase (29–52°) more than the clearing temperatures (13–38.5°) narrowing the total range over which mesophases occur from 49–92 to 43–87°. Except for the unknown biaxial smectic phase found in the OR' series, the same types of mesophases were observed in the $OCOR'$ series. A comparison of the types of mesophases found for the various homologs in Table IX shows that the *N* phase begins at the same chain length (2C) in both series but persists to a longer one (8C) in the $OCOR'$ series where it also has a larger maximum range. This trend was also observed in the phenylbenzoates *Id* suggesting that the $OCOR'$ group is a more favorable substituent for observing the *N* phase than the OR' group. The *S_A* phase occurs at about the same chain length in both the OR' and $OCOR'$ series, but the much smaller maximum range once again indicates that this phase is less favored when $Y=OCOR'$ than when $Y=OR'$. As was true in the phenylbenzoates, the *S_C* phase enters the cyclohexane series at a longer chain length (12C) when $Y=OCOR'$ than when $Y=OR'$ (7C) and persists in longer chain lengths. The *S_C* phase is still present at 22C and the curve in Figure 3b suggests that it will probably exist at even longer chain lengths whereas extrapolation of the plot for the OR' series (Figure 3a)[†] suggests that the *S_C* phase will disappear at ~20C. How-

[†]The C_{18} homolog of this series has been prepared since the earlier report in Reference 7. Transition temperatures observed are as follows: 113.3° (*C-S_B*), 114.2–115.1° (*S_B-S_C*), 143.0–144.0° (*S_C-I*), and 94.9° (*S_B-C*).

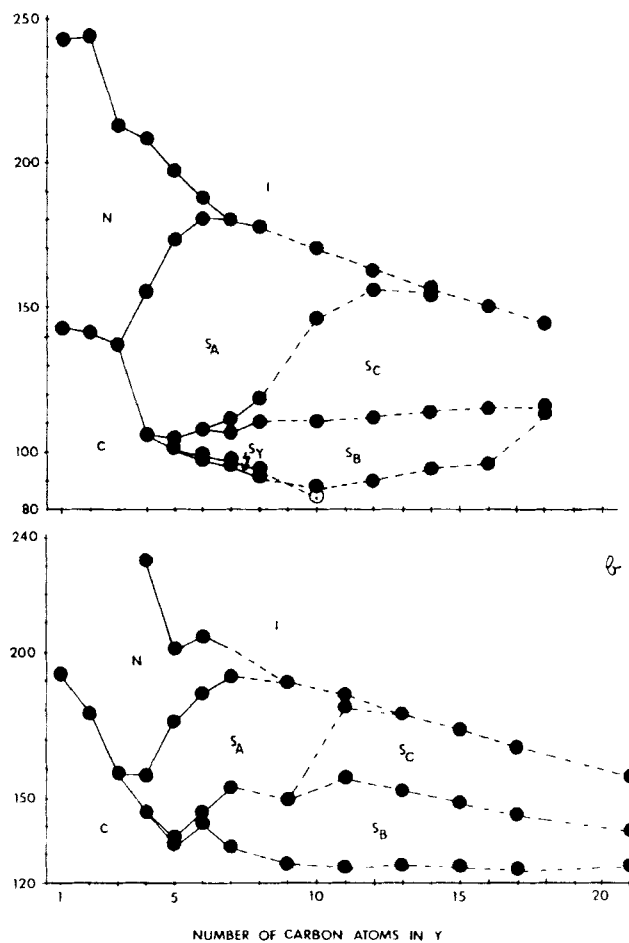
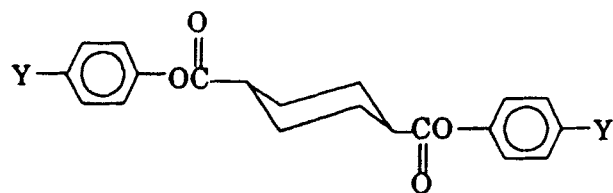
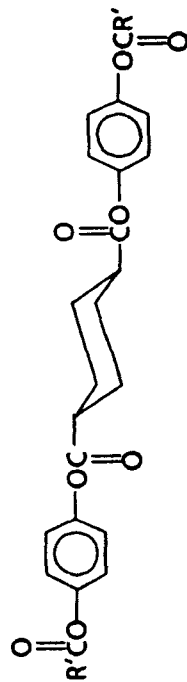


FIGURE 3 Transition Temperatures (°C) versus the Number of Carbon Atoms in Y for



- a. $Y=OR'$ (data from reference 7).
 b. $Y=OCOR'$

TABLE VIII
Transition Temperatures (°C) for



R'	C ^a	S _B	S _C	S _A	N	I
C ₁	161.8				191.5–192.2	>300 ^b
C ₂	158				178.2–179.5	>300
C ₃	147 ^c				158.4–158.6	>300
C ₄	133.5			142.6–145.3	157.5–157.7	231.4–231.5
C ₅	124.1	133.7–133.9	—	135.0–135.7	176.1–176.3	200.5–200.9
C ₆	128	140.4–140.7	—	144.8–144.9	185.4–185.5	205.4–205.5
C ₇	126.1	132.3–132.5	—	153.3–153.8	191.9–192.2	201.0–201.4
C ₉	114.5	126.1–126.6	—	149.2–149.3	—	189.4–189.5
C ₁₁	117.0	125.4–125.5	156.6–156.8	180.6–180.8	—	184.5–184.7
C ₁₃	118.0	125.6–125.8	152.2–152.3	—	—	177.9–178.2
C ₁₅	119.0	124.7–125.1	147.6–147.9	—	—	172.7–172.8
C ₁₇	120.0	123.8–124.1	143.7–143.8	—	—	167.3–167.8
C ₂₁	121.5	125.0–126.1	138	—	—	157.1–157.2

^aLetters are defined in the experimental section.

^bA clearing temperature was not obtained by 300°, the limit of our heating stage.

^cCrystal changes on heating, occurred at 146.7°, and 151.2–151.3°.

TABLE IX
Comparison of Mesophases for



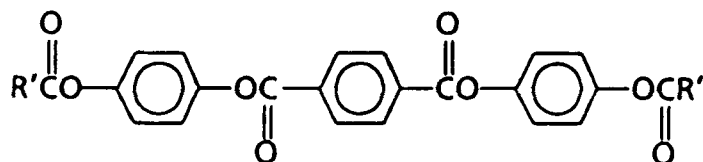
Mesophase	Chain lengths at which phase occurs ^a		Maximum Mesophase length (°C chain length)	
	Y=OR'	Y=OCOR'	Y=OR'	Y=OCOR'
N	2-6	2-8	103-2C	>142-4C
S _A	4-12	5-12	73-6C	41-6C
S _C	7-18	12-18	44-12C	26-14C
S _B	5-18	7-18	24-10C	31-12C

^aTotal number of carbon atoms in Y.

ever, unlike the phenylbenzoates, the phase length of the S_C phase is less when $Y=OCOR'$ than when $Y=OR'$. The S_B phase enters the $OCOR'$ series at a longer chain length (7C) than when $Y=OR'$ (5C) and as in the phenylbenzoates, it seems more favored having a wider phase length. However, it does not disappear at longer chain lengths as in the phenylbenzoates but still occurs at 22C and will probably still be present at even longer chain lengths. Although this phase is still present at 18C when $Y=OR'$, it has a short range and will probably disappear in the next homolog.

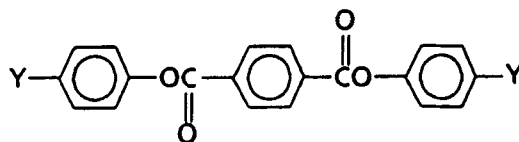
The entry of the S_C phase at 12C in the cyclohexane diesters **2b** again emphasizes the need to be careful in determining the smectic trends in a series at chain lengths <10C. The data for both $OCOR'$ series also emphasizes the problem of trying to compare mesomorphic properties for the same terminal chain lengths. Smectic phases can be just as favorable but require a longer chain length for some terminal substituents as compared to others. Thus comparisons of only one chain length in various series is not very useful. At least 2 chain lengths—one medium and one long—on both ends of the molecule are needed. Although two homologs often give the smectic trends in a particular series, homologous series plots are still more useful for making accurate comparisons between various series as these give a more complete picture and make it possible to compare any desired chain lengths. The additional synthesis work needed is, however, not always easy to justify.

Two of the acyloxy terphthalic acid diesters:



were also prepared by the method described in reference 8. Although the data are scanty, a comparison of the mesomorphic properties of these esters with those of the corresponding OR' series (Table X) indicates a trend towards higher transition temperatures and fewer smectic phases in the OCOR' series; a trend also seen in the cyclohexane series. A comparison of the effect of replacing the benzene ring with a cyclohexane ring in both the $\text{Y}=\text{OR}'$ series and OCOR' series (Table XI) on the transition temperatures indicates that the melting temperature is lowered by about the same amount in both series ($\sim 65^\circ$) and that this is considerably more than the lowering of the clearing temperature ($\sim 20^\circ$). A similar comparison of the mesophase lengths (Table XI) shows an increase in the total range for both cyclohexane series. The smaller ranges observed when $\text{Y}=\text{OCOR}'$ is evident. The S_C phase observed in the terphthalic acid series seems to disappear in the cyclohexane series but actually occurs

TABLE X
Transition Temperatures ($^\circ\text{C}$) for

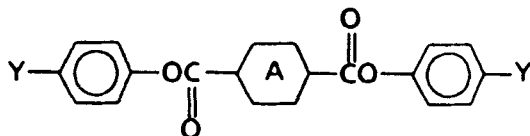


Y	C	S_C	S_A	N	I
C_5O	163.3	167.6	170.4	175.5	214.1 ^a
C_6O	155.3	161.8	177.5	182.1	208.3 ^a
C_7O	—	153	—	—	188 ^b
C_{10}O	141.9	145.8–147.0	—	174.2–175.1	178.3
OCOC_6	201.1	—	—	206.1–206.4	230.7–230.8
OCOC_9	187.6	191.4–191.9	—	199.9–200.3	208.1–208.4

^aData from Ref. 8.

^bData from Ref. 2. Only the melting and clearing temperatures ($\text{N} \rightarrow \text{I}$) were reported.

TABLE XI
Comparison of Mesomorphic Properties for



Y	$\Delta(T_{CH}-T_{CB})^a$ for	
	melting	clearing
OC ₅	-67	-21
OC ₆	-65	-20
OC ₇	-62	-8
OC ₁₀	-60	-8
OCOC ₆	-65	-25
OCOC ₉	-65	-19

Mesophase Length (°C) for									
CH					B				
Y	S _C	S _A	N	Total	S _B	S _C	S _A	N	Total
OC ₅	2.8	5.1	38.5	47.5	4	—	68	20	92
OC ₆	15.7	4.6	26.2	46.5	10	—	73	7	91 ^b
OC ₁₀	28.4	—	4.1	32.5	24	35	24	0	86 ^b
OCOC ₆	0	—	24.4	24.4	4.2	—	40.6	20	65.1
OCOC ₉	8.9	—	8.1	17.0	22.7	—	40.3	0	62.9

^aCH: A = cyclohexane; CB: A = benzene

^bAn unknown smectic phase was also observed.

at longer chain lengths at OC₁₀ and OCOC₁₁. The *N* phase is less favored in the cyclohexane esters whereas the *S_A* and *S_B* phases are definitely more preferred.

MESOPHASE AND TRANSITION IDENTIFICATION

Mesophases were identified primarily by the textures observed by hot-stage polarizing microscopy. Textures observed for the *N*, *S_A*, and *S_C* phases were typical of those usually seen for these phases (see Reference 7). In the cyclohexane diesters *2b*, the *S_B* phase was easily identified by its nice focal conic fan texture with transition bars at the transition to either the *S_C* or *S_A* phase. This was not true, however, of the *S_B* phase in the phenylbenzoates *1d*. In these esters, this phase

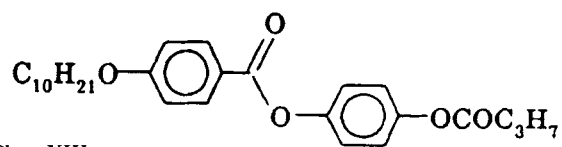
was usually of short range with its $S_B \rightarrow M$ transition very close to the melting transition. Many of the homologs which showed S_B phases had a $N-S_C-S_B$ sequence. Good fan textures are not always easily obtained in S_C phases which occur directly below a nematic phase (see reference 9) making it difficult to obtain a good fan texture in the S_B phase. Homeotropic textures in the N phase and schlieren textures in the S_C phase are also hard to obtain with a $N-S_C$ sequence making it difficult to obtain a good homeotropic texture for conoscopic studies in the S_B phase. However, even when the S_B phase occurred below a S_A phase ($X_1=C_{10}O$, $R'=C_3, C_4$) in which a good homeotropic texture was observed, cooling this texture gave a gray mosaic one rather than a good homeotropic texture making it difficult to obtain a good uniaxial cross. Yet the cover slip could be moved in the S_B phase and occasionally it was possible to obtain a small homeotropic area good enough to suggest this phase was a uniaxial one. Similar problems were encountered earlier with the S_B phase in the phenylthiobenzoates which was shown to be a crystalline S_B phase by x-ray crystallography studies.^{10,11}

The identification of this S_B phase by microscopy was made more difficult by the similarities of its textures with those observed for crystals. Cooling a good fan texture obtained in the S_A phase of the C_3 homolog ($X=C_{10}O$, Figure 4) caused the growth of sharp spears similar to the growth pattern often seen for a crystalline phase (Figure 4a). Continued cooling gave the texture shown in Figure 4b, which could be mistaken for a crystalline phase. However, some areas of the sample had a more smectic-like appearance (Figure 5) with a texture that has a resemblance to the lancets reported by Demus and Richter for a S_B phase occurring below an isotropic liquid.¹² This texture gradually became more of a gray mosaic one on standing (Figure 6) probably due to its tendency to form the homeotropic texture but with poor alignment to the slide. Some of these textures resemble those reported by Gray and Goodby for S_B phases occurring below very short range smectic phases¹³ and the small S_A phase is probably the reason why the S_B textures differ from those usually observed.

For those homologs in which the S_B phase occurred below a S_C phase, the growth pattern often appeared as a moving front of concentric arcs which was easier to photograph in a mixture (Figure 7). These arcs disappeared quickly suggesting that they are transition bars. The remaining texture often had a feathery appearance (Figure 8) which also resembles textures sometimes observed in crystalline phases.



FIGURE 4 Growth of S_B spears in the S_A phase at 72.2° (magnification = 10×20) of



See Color Plate XIII

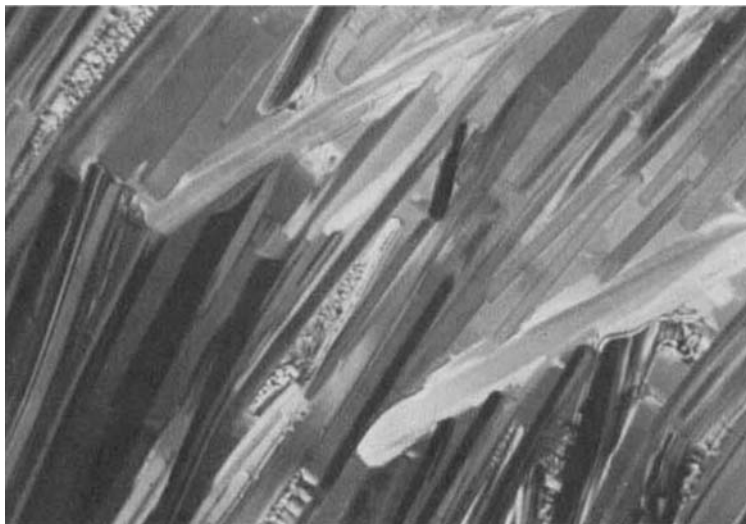
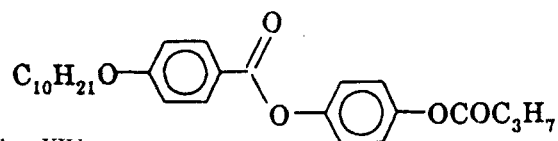


FIGURE 5 Microscopic Texture for S_B Phase at 68.4° ($M = 10 \times 16$, different area from that in Figure 4) in

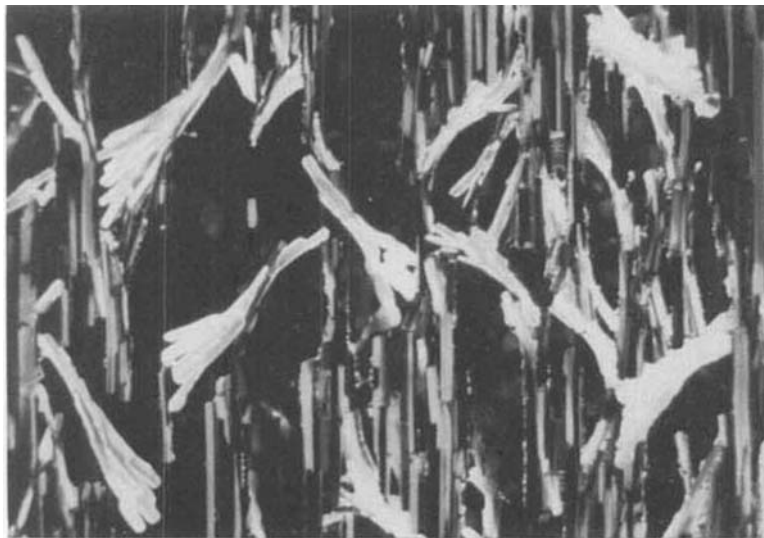
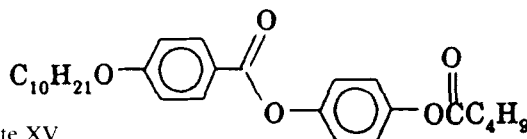


See Color Plate XIV

Another problem in determining if a S_B phase was present was the observation of crystal-crystal changes preceeding the C - S_B transition. At times, different melting temperatures were observed but these could not be determined with any degree of repeatability. Some homologs also crystallized very slowly so that all melted samples were allowed to set for at least 24 hours before they were heated to obtain the C - S_B transition.

Additional support for the S_B identification was obtained from a mixture study using the contact method¹⁴ with the acyloxy ester *Id* ($R=C_{10}$, $R'=C_6$) and the dialkoxy ester *1b* ($R=C_{10}$, $R'=C_6$) which has been reported to have a S_B phase.¹⁵ No interface was observed between the two S_B phases.[†] The S_B structure for the acyloxy ester was confirmed by x-ray diffraction studies which indicated that this

[†]Care must be taken in interpreting such results, however, as a small region of immiscibility can go undetected, as was true of the tilted S_B phase now known to be S_H phase in TBBA (see references 16 and 17).

FIGURE 6 Microscopic Texture for S_B Phase at 68.4° ($M = 10 \times 10$) in

See Color Plate XV

is a crystalline S_B phase with Bragg spacings of $d(S_B) = 34.5 \text{ \AA}$ and $d(S_C) = 30.2 \text{ \AA}$. An earlier x-ray study of the dialkoxy diester **2a** ($R=C_8$) reported that the S_B phase in this ester was also crystalline.¹⁸ The obvious presence of transition bars in the acyloxy series **2b** also suggests that the S_B phase is a crystalline one in this series.

At longer chain lengths ($R'=C_{11}$ - C_{21}) for which no S_B phases are reported in Table V, the bright birefringent S_C phase turned to a predominately black-gray mosaic texture with little birefringence on cooling to the crystalline phase. Such a crystalline phase is so rare that this phase was initially thought to be a S_B phase, especially since a gray mosaic texture was often observed for this phase in the shorter homologs. However, reheating this texture gave a transition back to the S_C phase at a higher temperature than that observed on cooling, i.e. the S_C phase had supercooled to form the dark mosaic texture and therefore this is probably the texture for a crystalline phase. The large increase in birefringence observed at the melting transition made this one easier to observe than those in the shorter homologs. When these black crystals were allowed to set for a long time, they became

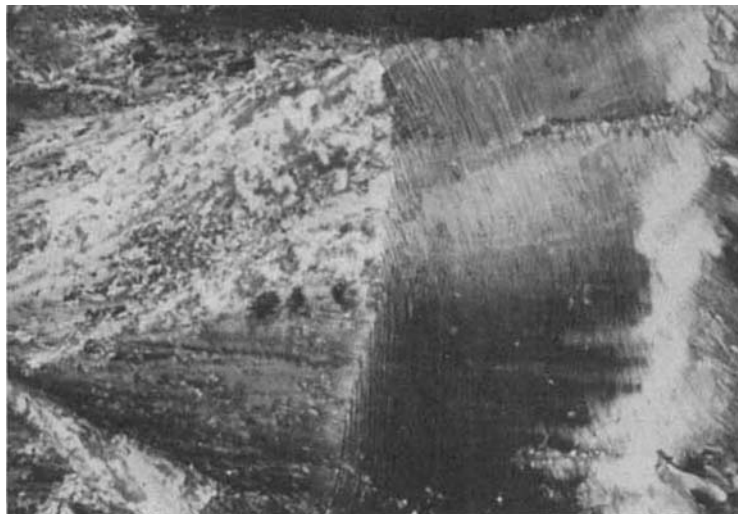
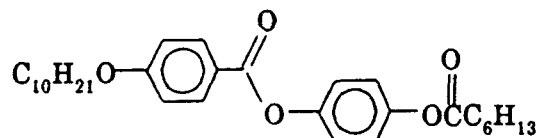
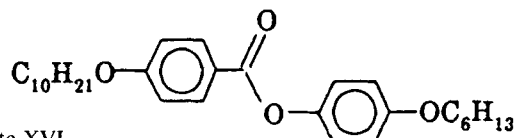


FIGURE 7 Microscopic Texture ($M = 10 \times 10$) at the growing front of the S_B phase in



(on the right) in a mixture with the S_C phase of



See Color Plate XVI

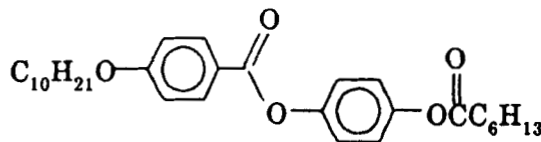
more birefringent making the transition to the S_C phase much more difficult to see.

DSC scans were obtained for those homologs of the phenylbenzoates *Id* ($R=C_{10}$) in which the transitions in the melting region were questionable. Several problems were encountered in interpreting these curves:

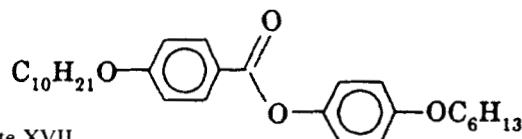
1. The $S_B \rightarrow M$ transition was often close to the $C \rightarrow S_B$ transition and had a large ΔH value, sometimes larger than that for the melting transition (Figure 7a).
2. As in the microscopic studies, some samples crystallized slowly and the first crystallization sometimes had a very low ΔH value.



FIGURE 8 Featherly Texture of the S_B phase ($M = 10 \times 10$) in



(on the right) in a mixture with the S_C phase of



See Color Plate XVII

3. Various crystal forms were observed as shown by the differences in the melting from fresh and recrystallized crystals.

For example, the scan for the $R'=C_2$ homolog (Figure 9†) shows a broad $C \rightarrow S_B$ peak at 69.1° overlapping with the sharp $S_B \rightarrow N$ peak at 70.5° when fresh crystals were heated at $2.5^\circ/\text{min}$ (Figure 9a). Cooling the isotropic liquid gave a sharp peak for the $N \rightarrow S_B$ transition but no crystallization by 40° (Figure 9b). This sample was allowed to

†Typically, temperatures on the DSC scans differed from those obtained by microscopy. Since the microscope temperatures are more accurate, these are used throughout this discussion and were also used to estimate transition temperatures observed only by DSC and to calculate the ΔH values. Some of the microscope temperatures have been added to the DSC curves for the convenience of the reader.

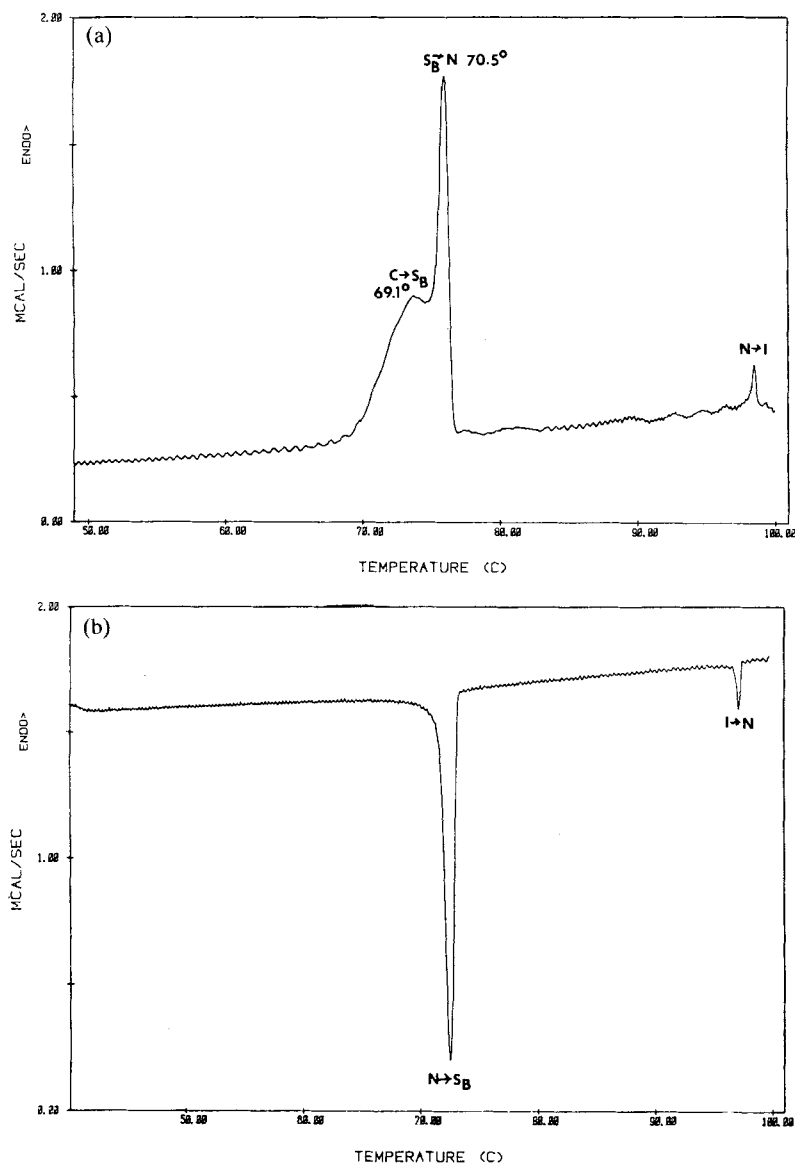
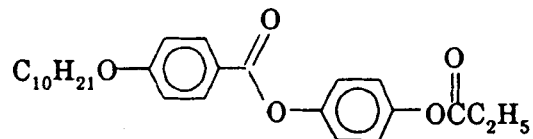


FIGURE 9 DSC Scans for



a. heating; b. cooling; c. reheating after setting at RT for 24.5 hr.

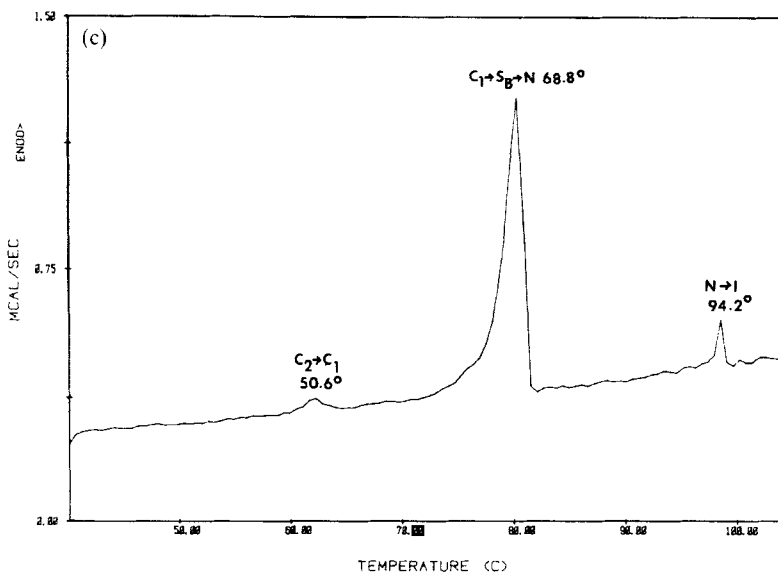
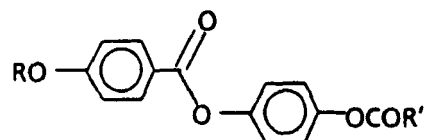


FIGURE 9 (continued)

set for 24 hours and then reheated to give a weak broad $C_2 \rightarrow C_1$ transition at 50.6° (Figure 9c) and an unresolved broad intense peak at 68.8° . This suggests two slightly different melting temperatures. The ΔH values calculated from the peak areas indicate that the $S_B \rightarrow N$ transition involves a larger heat change than the $C \rightarrow S_B$ transition (see Table XII). This suggests that the structure of the S_B phase is much more like that of the crystalline phase from which it is formed than that for the S_C phase. When fresh crystals of the $R' = C_3$ homolog were heated, a large broad absorption was observed at 58.0° (Figure 10a). A small broad peak at 65.4° preceded the $S_B \rightarrow S_A$ transition at 73.0° . This small peak supercools by ca. 1.7° suggesting it is a crystal-crystal change (Figure 10b). It also occurs at the crystallization temperature observed by microscopy. However, since the peak at 58° has a much larger ΔH value, suggesting it is the melting transition, the possibility that this small peak could represent a transition to a more highly ordered smectic phase that supercools slightly cannot be eliminated. The C_3 homolog is the only one in this series which showed this behavior and the small ΔH value for the melting transition in the C_2 homolog lends support for assigning this small transition in the C_3 homolog as the melting one. When this sample was allowed to set at room temperature for 23 hours and reheated, only a broad


TABLE XII
Thermodynamic Data Obtained from DSC for



R	R'	Temperature (°K) ^a	ΔH (KJ/mole)	ΔS (J/mole/°K)	Transition Type
C ₁₀	C ₂	342.2*	3.81	11.13	C _{fresh} →S _B
		342.0			
		323.8*	0.75	2.32	C ₂ →C ₁
		342.0	22.0	64.3	C ₁ →S _B
		343.6	15.5	45.1	S _B →N
	C ₃	367.2	0.96	2.6	N→I
		331.2	20.8	62.8	C ₂ →C ₁
		338.6	0.75	2.2	C ₁ →S _B
		344.6	22.8	66.2	S _B →S _A
		346.2	0.38	1.10	S _A →N
		370.6	1.30	3.5	N→I
	C ₄	338.6	24.0	70.9	C→S _B
		341.4	13.6	39.8	S _B →S _A
		346.6	0.71	2.1	S _A →N
		367.2	1.22	3.3	N→I
		325.2	13.8	42.4	S _B →C
	C ₆	343.1	32.4	94.4	C→S _C
		353.6	0.84	2.4	S _C →N
		365.4	1.55	4.2	N→I
		341.8	15.1	44.1	S _C →S _B
	C ₈	342.2	33.4	97.6	C→S _C
		364.1	1.84	5.1	S _C →N
		369.6	2.26	6.1	N→I
		334.1	7.84	23.4	S _C →S _B
		312.2	14.66	47.0	S _B →C
C ₁₀	C ₁₁	342.2	48.5	141.7	C→S _C
		366.2	2.26	6.2	S _C →N
		368.2	4.27	11.6	N→I
		330.8	43.1	13.0	S _C →C
	C ₁₃	368.6	140.5	381.2	C→S _C
		347.2	27.6	79.5	S _C →I
		341.0	137.8	404.1	S _C →C
	C ₁₇	356.0	151.72	426.18	S _C →C
		367.2	25.30	68.90	S _C →I
	C ₁₂	~337.4	47.9	142.0	C _{fresh} →S _B →S _C
		~337.4	23.5	69.6	C _{recryst} →S _B →S _C
		355.6	0.88	2.47	S _A →N
		367.0	1.34	3.65	N→I
		339.0	6.95	20.5	S _C →S _B
		273.2*	1.26	4.61	S _B →C(?)
		330.4*	0.25	7.60	C-C

TABLE XII (cont.)

Thermodynamic Data Obtained from DSC for

R	R'	Temperature (°K) ^a	ΔH (KJ/mole)	ΔS (J/mole/°K)	Transition Type
		324.6	1.22	3.80	C-C
	C ₆	~344.0	29.7	86.3	C _{fresh} →S _B
		347.2	8.09	23.2	S _B →S _C
		~370.0	9.01	24.4	S _C →N→I
		319.2*	59.5	186.4	S _B →C
		338.8*	1.76	5.19	C ₂ →C ₁
		345.4*	20.32	58.8	C ₁ →C _B →S _C
		370.0	7.92	21.4	S _C →N→I
					
		398.6	38.8	97.3	C→S _B
		430.0	8.34	19.4	S _B →S _C
		458.0	9.09	19.8	S _A →I
		398.6	28.8	72.2	S _B →C

^aTemperatures used were those obtained by microscopy unless indicated by an asterisk. These were estimated from DSC scans using a transition observed by microscopy as a standard.

intense peak was observed for these three transitions (Figure 10c) which also indicates the presence of more than one crystalline form and two melting transition temperatures. The $S_A \rightarrow N$ transition could not be seen in the heating scans (Figures 10a and c) even though microscopy indicated this transition was an enantiotropic one. It was observed in the cooling curve (Figure 10b) but only as a very weak and broad peak near the much larger $S_A \rightarrow S_B$ peak. This suggests that it was just not possible to detect it on the heating scan.

DSC scans of the remaining homologs presented no new problems. These scans indicated that the S_B phase was enantiotropic in the $R'=C_4$ homolog, monotropic in the C_6 one and no longer present in the C_8 or longer homologs. These curves were relatively easy to interpret. A scan for the C_4 homolog with $R=C_{12}$ (Figure 11) was, however, not so easily interpreted. This was not surprising as the transitions in the melting region were also difficult to determine from microscopic textures. The DSC heating scan for the C_4 homolog (Figure 11a) shows a broad melting transition on heating the fresh crystals. When this sample was cooled, an intense peak corresponding to the $S_C \rightarrow S_B$ transition observed by microscopy followed within a few degrees by a weaker but fairly sharp peak at $\sim 63^\circ$ and then 2 weak

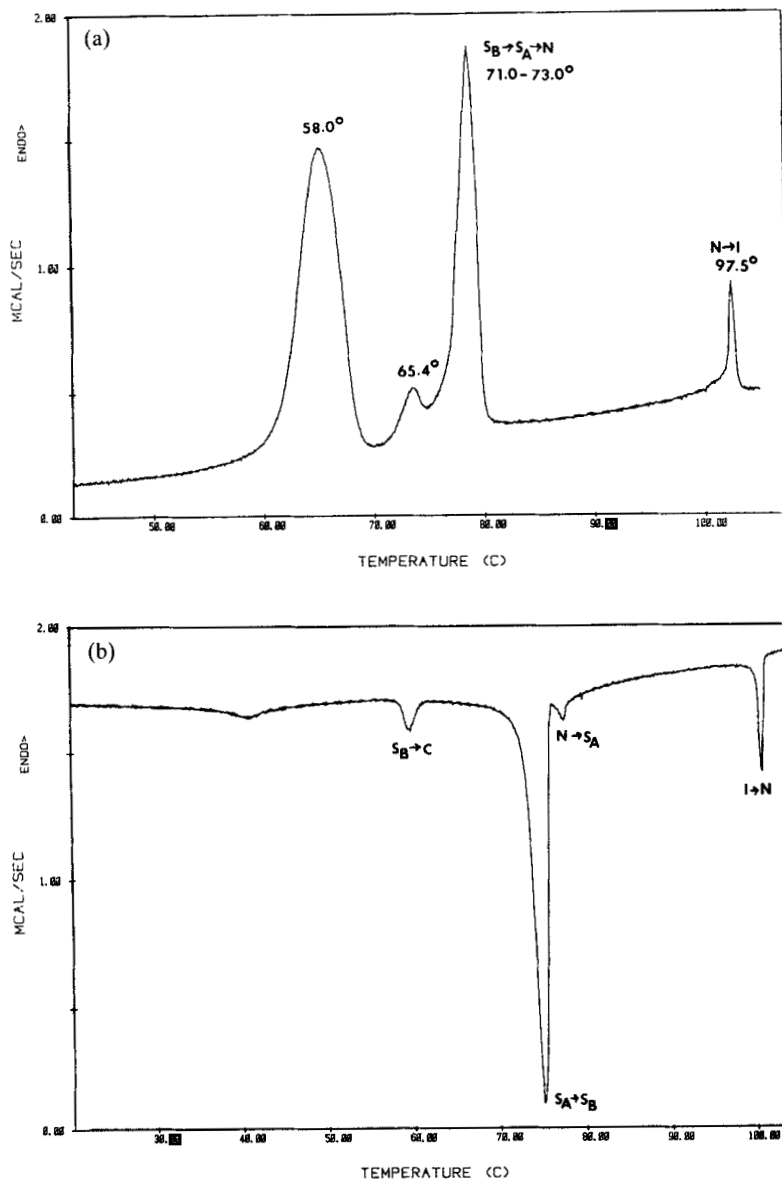
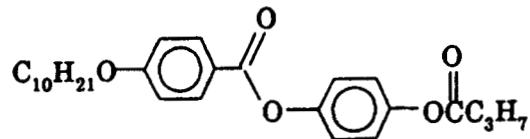
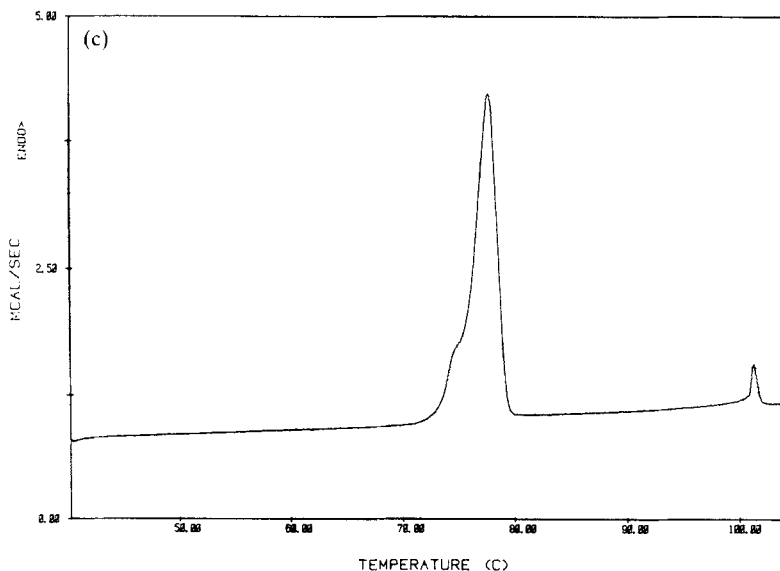


FIGURE 10 DSC Scans for



a. heating; b. cooling; c. reheating after setting at RT for 24 hr.

FIGURE 10 (*continued*)

broad peaks (Figure 11b). The peak at $\sim 63^\circ$ could represent a transition to a monotropic more ordered smectic phase or it could be the crystallization transition. The temperature for this transition could not be determined by microscopy. When this sample was allowed to set for ~ 47 hours and reheated, a broad peak was again observed for the melting transition, but there seemed to be some resolution between a peak at 64° and a shoulder at 66° (Figure 11c). The shoulder corresponds to the S_B - S_C peak observed on cooling, confirming that the S_B phase is enantiotropic. The melting region for the $R'=C_9$ homolog was straightforward, but the S_C - N and N - I transitions occurred as a single peak; their temperatures being too close to resolve at a heating rate of $2.5^\circ/\text{min}$.

The DSC scan for the cyclohexane diester **2b** with $R'=C_{11}$ showed no anomalies agreeing with the microscope data. All the thermal data obtained from DSC scans of the compounds studied are presented in Table XII. Although the combination of DSC and microscopy data made it possible to convincingly identify the transitions in the melting region in these esters, the difficulties encountered were enough to humble any experienced liquid crystal microscopist to the point of being unwilling to identify any texture or transition with absolute certainty.

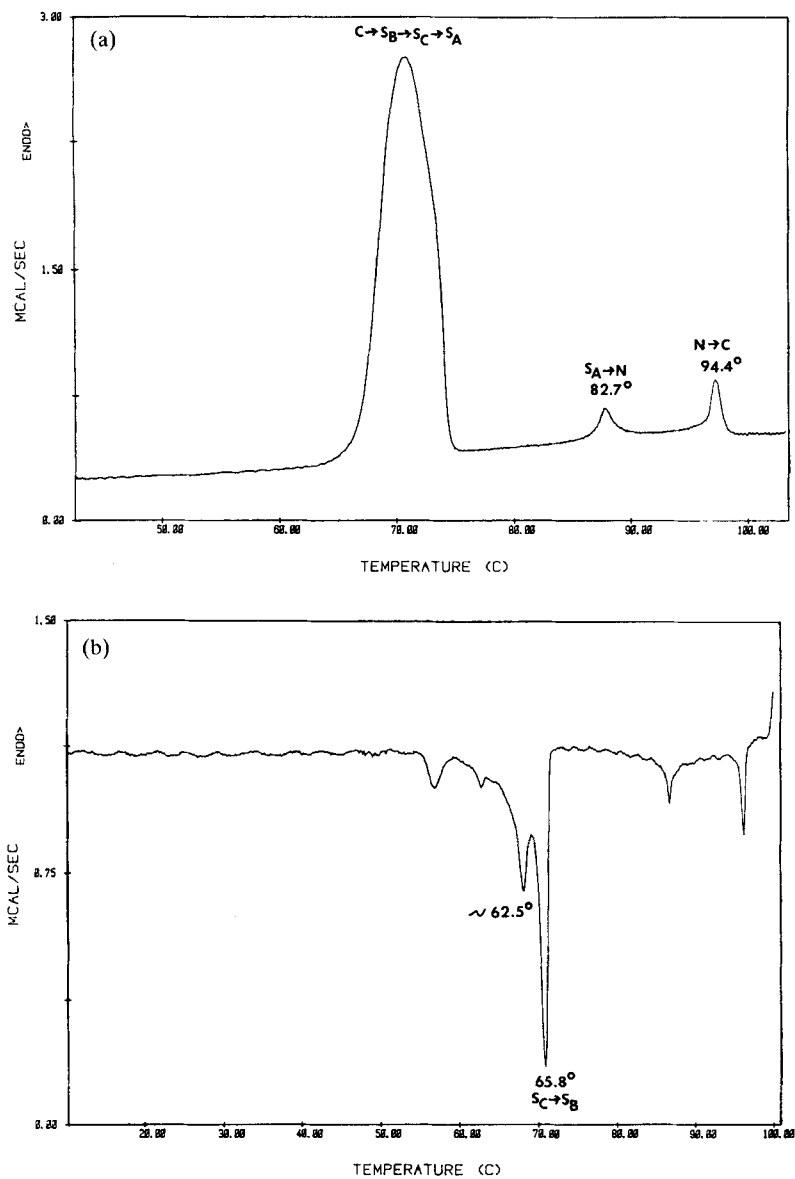
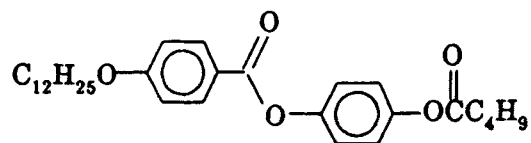


FIGURE 11 DSC Scans for



a. heating; b. cooling; c. reheating after setting at RT for 46.5 hr.

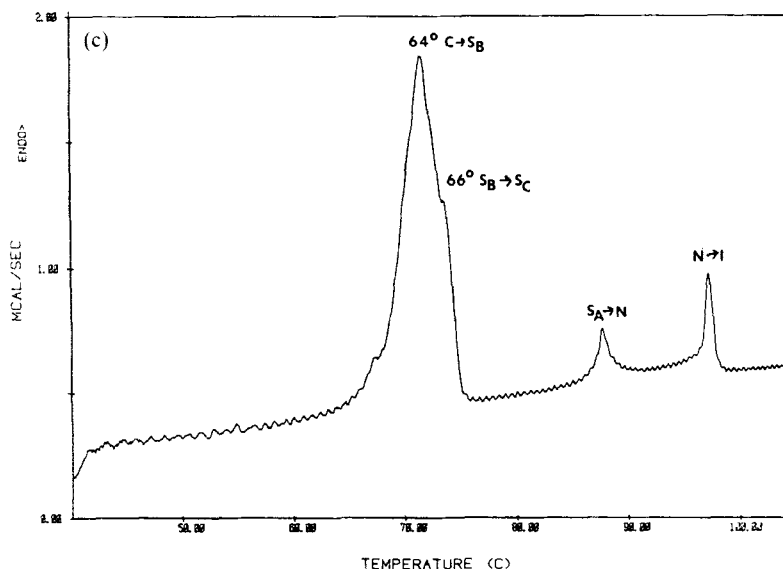


FIGURE 11 (continued)

DISCUSSION

A variety of parameters are of interest when studying the relationships between molecular structure and mesomorphic properties:

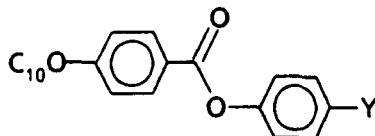
1. transition temperatures,
2. width of temperature range over which mesophases occur,
3. types of mesophases,
4. width of temperature range for specific mesophases,
5. chain length at which specific mesophases occur.

Mesomorphic properties for the phenylbenzoates *1* and the cyclohexane diesters *3* have now been determined for four different phenolic carbonyl containing substituents making it possible to make some preliminary comparisons of the effect of these substituents on mesomorphic properties.

A comparison of the melting and clearing temperatures for three different chain lengths of these four substituents in the phenylbenzoates *1* (X=RO) in Table XIII indicates that these temperatures increase in the order:

$$R < OR' \leq OCOR' < COR'$$

TABLE XIII
Comparison of Melting and Clearing Transition Temperatures (°C) for



Chain Length ^b	Temperature Range ^a for Y=			
	R'	OR' ^c	OCOR'	COR' ^d
5	55–69 ^d	64–89	66–98	93–121
8	53–73 ^f	71–88	70–92	106–121
10	62–76 ^g	74–91	69–95	108–121
Differences				
5	9, 20	2, 9	27, 23	
8	18, 15	1, 4	36, 29	
10	12, 15	–5, 4	39, 26	

^aTemperatures were rounded off for convenience and do not include those for monotropic phases.

^bThe total number of atoms in the terminal chain backbone. See the discussion section.

^cData from Ref. 2.

^dData from Ref. 1.

^eData from Refs. 2 and 5.

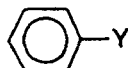
^fObtained by estimation using a plot of data obtained from Refs. 2 and 5.

^gData from Ref. 5.

which is the same order observed for increasing dipole moments of the same type of substituents on the benzene ring (Table XIV). Even the magnitudes of the differences are similar. Thus, it appears that the larger the dipole moment of this terminal chain in the phenylbenzoates, the higher the transition temperatures are. This trend also seems to occur in the cyclohexane diesters 2 (Table XV) but is broken by the lower temperatures observed when Y=COR' giving the following order:



A comparison of the number of mesophases observed for these substituents in both series (Table XVI) shows some interesting trends.

TABLE XIV
Dipole Moments for

Y	$\mu(\text{CCl}_4)^a$
Me	0.35–0.40
OMe	1.24–1.32
OCOMe	1.50–1.65
COMe	3.00

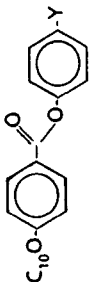

^aData from Ref. 19.TABLE XV
Comparison of Melting and Clearing Transition Temperatures (°C) for

Chain Length ^b	Temperature Range a for Y=			
	R' ^c	OR' ^d	OCOR' ^e	COR' ^e
5	95–154	107–209	150–>300	144–202
8	71–140	95–180	141–206	109–193
10	66–135	87–174 ^f	130–195 ^g	105–190

Chain Length ^b	Differences		
	R' – OR'	OR' – OCOR'	OCOR' – COR'
5	12, 55	52, >91	–15, > –98
8	24, 40	46, 26	–32, –13
10	21, 39	43, 21	–25, –5

^aTemperatures were rounded off for convenience and do not include those for monotropic phases.^bThe total number of atoms in the terminal chain backbone. See the discussion section.^cData from Ref. 8.^dData from Ref. 7.^eData from Ref. 1.^fEstimated from Figure 3a.^gEstimated from Figure 3b.

TABLE XVI
Types of Mesophases Observed

Ester Type	R'	OR'	OCOR'	COR'
	S _A , N	S _B , S _C , S _A , N	S _B , S _C , S _A , N	S _A
	S _B , S _A , N	S ₇ , S _B , S _C , S _A , N	S _B , S _C , S _A , N	S _C , N

Except when $Y=OCOR'$, one more mesophase was observed in the cyclohexane diesters than in the phenylbenzoates. More mesophases were found in esters with the alkyl chain (R') connected to the phenolic ring through an oxygen atom with ($OCOR'$) or without (OR') an intervening carbonyl group than were observed when the connection was made through a carbon atom whether or not it contained a carbonyl group (COR' , R'). The order of increasing number of mesophases observed in both series:

$$COR' < R' < OCOR' \leq OR'$$

has no correlation with the order of increasing dipole moments of these substituents suggesting that these do not determine the number of mesophases observed.

A comparison of the maximum mesophase temperature ranges[†] for these two series (Table XVII and XVIII) indicating that these ranges increase in the following orders:

Series 1: $R' < OCOR' \approx COR' < OR'$

Series 2: $R' < COR' < OR' < OCOR'$

with little agreement between the two series. A similar comparison of the maximum total smectic phase ranges:

Series 1: $R' < OCOR' < COR' < OR'$

Series 2: $OCOR' < R' < COR' < OR'$

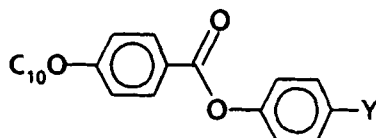
gives a better correlation between the two series. These data also show that although the smallest number of smectic phases are found when $Y=COR'$, this one has the widest single phase range.

A comparison of the types of mesophases observed in both series (Table XVI) also shows some interesting trends. No tilted phases occur in either series when $Y=R'$. The same types of mesophases were observed in both series (S_A , N) with an additional smectic phase (S_B) occurring in the cyclohexane diesters. This is also true when $Y=OR'$ but both tilted and non-tilted phases were found. When $Y=OCOR'$, the types of mesophases were the same and included both tilted and non-tilted smectic phases. However, when $Y=COR'$ a total conversion occurred from the uniaxial S_A phase to the biaxial tilted S_C phase. Again an additional phase (N) was added in the

[†]There is a problem in making this comparison since not all the homologs were prepared in all these esters so the actual maximum in a series might not have been reported. However, plots of available data suggest that either the maxima have been reported or will not vary appreciably from them.

TABLE XVII

Maximum Mesophase Ranges (°C) for



Mesophase	Y			
	R' ^a	OR' ^b	OCOR'	COR' ^c
N	4.5	10.6	24.5	0
S _A	15.6	16.2	5.3	29.4
S _C	0	16.1	23.8	0
S _B	0	() ^d	6.6	0
Total M	15.6	45	29.1	29.4
Total S	15.6	39	23.8	29.4

^aCalculated using data from Ref. 20. Data for all members of this series are not available.

^bCalculated using data from Ref. 2 and 5.

^cCalculated using data from Ref. 9. Data for all the members of this series are not available, but a plot of the available data suggests this is the maximum.

^dMonotropic phase only.

TABLE XVIII

Maximum Mesophase ranges (°C) for



Mesophase	Y			
	R' ^a	OR' ^b	OCOR'	COR' ^c
N	58	103	>142	82
S _A	34	73	41	0
S _C	0	44	26	86
S _B	63	24	31	0
Total	83	103	>142	91
Total S	83	92	63	86

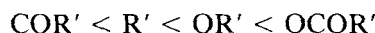
^aCalculated using data from Ref. 8.

^bCalculated using data from Ref. 7.

^cCalculated using data from Ref. 1. Data are not available for all members of this series.

cyclohexane diesters.[†] At this time, it is difficult to explain these trends.

Another structural feature to be considered is the steric hindrance between the Y substituent and the hydrogen atoms *ortho* to it on the benzene ring. It is known that if steric hindrance is too great, mesomorphic properties are not observed due to the increased bulkiness of the molecule in this area which is believed to affect the packing of the molecules in a parallel manner in the mesophase.³ A comparison of molecular models of benzene containing these four substituents (Figure 10) shows that this steric hindrance increases in the following order:



Since mesophases were observed when $\text{Y}=\text{OCOR}'$, the steric hindrance is not large enough to cause the loss of mesomorphic properties as is true when $\text{Y}=\alpha$ -methyl alkyl group. However, it still can affect the packing of the molecules in two ways. As the steric hindrance increases, overlapping of the π electrons of the benzene ring with electrons in the Y substituent decreases as the coplanarity of these two groups decrease. This decreases the lateral dipole moment of the substituent and polarizability of the molecule. The strength of this dipole moment is believed to be the major factor in determining whether a crystalline or hexatic S_B phase is observed in biphenyl esters; the crystalline S_B being favored by a weak dipole whereas the hexatic S_B is favored by a strong one.²¹ Terminal dipoles are also considered to be important in the formation of S_C phases.²² Although there is a strong lateral dipole in the esters 1 and 2 when $\text{Y}=\text{COR}'$, no hexatic S_B phases were observed. Smectic C phases occurred with this substituent in the cyclohexane diesters 2 but not in the phenylbenzoates 1. This phase was, however, prevalent when the Y substituent was attached to the benzene ring through an oxygen atom in agreement with a variety of mesogens containing two terminal alkoxy substituents.

Models indicate that there is no problem with either the R' or COR' substituents being coplanar with the benzene ring, a possible steric hindrance begins when $\text{Y}=\text{OR}'$. Experimental results disagree as to whether the methoxy group is coplanar with the benzene ring in anisole. Dipole moments suggest it is not²³ whereas NMR studies

[†]N phases do occur in shorter chain lengths in series 1.

suggest that it is (both in solution).²⁴ Models indicate that the substituent OCOR' cannot be coplanar with the benzene ring and studies on phenylacetate and similar structures agree with the angle to the plane estimated at 80–90°. ²⁵ This would increase the bulk of the OCOR' group near the benzene ring but models indicate that this is not enough to extend beyond the molecular volume of either of the ester series studied. Goodby has proposed that holes or spaces within the molecular envelope created by such bumps can be used in close packing arrangements to give the more highly ordered S_B and S_E phases.²⁶ Perhaps this is why the S_B phase is more prevalent in the esters 1 when $Y=OCOR'$. He also suggested that the more unsymmetrical the molecule, the more a S_B phase is favored. Although this seems to apply to the phenylbenzoates, the S_B phase is highly favored in the symmetrical cyclohexane diesters 2 as well. In this series, the S_B phase has a wider maximum range when $Y=OCOR'$ than when $Y=OR'$ as expected by considering the bulkiness of these substituents but it is twice this large when $Y=R'$. Of course, an unsymmetrical cyclohexane diester may be even more favorable for observing a S_B phase.

Steric hindrance between the Y substituent and the *ortho* hydrogen atom affects rotation around the aromatic carbon-Y bond in two ways. The increased bulk simply decreases rotation but the decrease in coplanarity causes a decrease in electron overlap and therefore a decrease in double bond character which would give a more flexible single bond character in some of these substituents. NMR studies on mesophases have shown that the order in the first few carbon atoms in a terminal chain determines the order in the remainder of the chain until the last three carbon atoms which are less ordered.²⁷ Usually in a homologous series, mesomorphic properties are lost when the alkyl chains become too long to maintain the rigid rod-like structure.⁶ The increased rigidity of the OCOR' near the phenolic ring caused by the steric hindrance with the *ortho* hydrogen atoms could explain why the S_C phase continues to occur at much longer chain lengths in both series when $Y=OCOR'$ than when $Y=OR'$. It also provides an explanation for the very high clearing temperatures observed in the short chain homologs with this substituent.

Still another factor to consider is the direction of the dipole moment of the Y substituent. The angle of the dipole to the benzene ring (which bisects the bond angle) is smaller in the OR' compounds (bond angle $\sim 110^\circ$) than in the COR' and OCOR' analogs† (bond angle

†The dipole moment has been shown to be along the C=O bond.²⁸

$\sim 120^\circ$) but it is not known how this would affect the mesomorphic properties.

Subsequent papers will provide data for additional phenolic and acid substituents with carbonyl-containing groups. It will be interesting to see how these groups fit into the trends already observed.

EXPERIMENTAL

The Pd-C catalyst was obtained from Matheson Coleman and Bell or Strem Laboratories; the latter being more reactive. The ligroine used had a bp of $60\text{--}90^\circ$. The elemental analysis was obtained from Spang Microanalytical Laboratories, Eagle Harbor, Michigan.

TLC data were obtained using Anal-Tech Silica Gel GHLF Uniplates[®] with CHCl_3 as the solvent and UV light as the detector. Melting points ($^\circ\text{C}$) were determined using a Hoover-Thomas melting point apparatus and are corrected. IR spectra were obtained using either a Perkin-Elmer 700 or a Pye Unicam 3-200 instrument. NMR spectra were determined using a Varian EM 360 (E) or FT80 (F) instrument in either deuterated chloroform (CD) or carbon tetrachloride (CT) with TMS as an internal standard. Transition temperatures ($^\circ\text{C}$) were determined using a Leitz-Ortholux or Laborlux 12 Pol polarizing microscope fitted with a modified and calibrated Mettler FP-2 heating stage at a heating rate of $2^\circ/\text{min}$ as described in Reference 29. Abbreviations used for phases are C = crystal, M = mesophase, S = smectic, S_E = smectic E, S_B = smectic B, S_C = smectic C, S_A = smectic A, N = nematic, and I = isotropic liquid. Monotropic phases are indicated by parentheses. Samples were cooled until they crystallized so that no monotropic phases would be missed unless otherwise noted. DSC scans were obtained at a rate of $2.5^\circ/\text{min}$ using a Perkin Elmer DSC 2 instrument interfaced with a model 3600 data station. Photographs of microscopic textures were taken using a Leitz 35mm camera and Ektachrome 160 film. Microscope transition temperatures for the ester *1b* ($R=\text{C}_{10}$, $R'=\text{C}_{14}$) are as follows: $84.8\text{--}85.7$ ($C\rightarrow S_C$), $90.7\text{--}91.1$ ($S_C\rightarrow I$), and 72.7° ($S_C\rightarrow C$).

4-Benzyloxy-*n*-nonanoyloxybenzene, **5** ($R'=\text{C}_9\text{H}_{17}$).

To a stirred soln of 20.0g (0.10 mole) of 4-benzyloxyphenol in 100 ml CH_2Cl_2 containing 13.8 ml Et_3N at RT was added dropwise, a soln of 18.0g (0.10 mole) of decanoyl chloride in 40 ml CH_2Cl_2 . The rxn mixture was stirred at RT for 1 hr and then washed with 150 ml

each of H₂O, 5% aq KOH, and H₂O. The organic layer was dried over anhyd Na₂SO₄, filtered, and the solvent removed from the filtrate *in vacuo* to give 45g (129%) of a light yellow solid. Recrystallization of this material 3× from ligroine gave 23.4g (68.8%) of the desired ester 5 (R=C₈H₁₇): mp 71–74°, TLC showed one spot with R_f=0.76 (R_f for 4 = 0.21) and IR (CHCl₃) 1750 (str CO₂R'), 1600 (wk Ar), and 1500 cm⁻¹ (str Ar).

4-Benzoyloxy-n-behenoyloxybenzene, 5 (R'=C₂₁H₄₃).

To a soln of 17.0g (0.05 mole) of behenic acid, 250 mg 4-N,N-dimethylpyridine and 10.0g (0.05 mole) of 4-benzoyloxyphenol in 150 ml CH₂Cl₂ was added 10.9g (0.05 mole) N,N-dicyclohexylcarbodiimide (DCC) and then the mixture refluxed for 6 hr. Chloroform was added to keep the product in soln during filtration to remove DCU. The filtrate was extracted with 100 ml each of 5% aq KOH and H₂O, dried over anhyd Na₂SO₄, and filtered. Concentration of this filtrate to half its volume by boiling and then cooling allowed for crystallization of the product to occur. The resulting crystals were collected by filtration to give 16.5g (74.3%) of the crude product. Recrystallization of this material from ligroine gave 4.7g (18.0%) of the purified ester 5 (R=C₂₁H₄₃): mp 95–96°, TLC showed one spot with R_f=0.53 (R_f for 4=0.07) and IR (Nujol) 1760 (str, CO₂R'), 1600 (wk, Ar), and 1500 cm⁻¹ (str, Ar).

The phenylbenzoates *1c* and *d* and cyclohexane diesters *2b* were prepared in the same manner. As reported earlier,⁷ the cyclohexane diacid chloride is very sensitive to moisture and must be stored in a vacuum or prepared *in situ*. Infrared data for these esters are as follows: *1c* 1730 (str, COR' + CO₂Ar), 1610 (wk, Ar), and 1490 cm⁻¹ (med Ar); *1d* 1750 sh (CO₂R'), 1730 (str, CO₂Ar), 1600 with sh at 1580 (str Ar) and 1500 (med Ar), and *2b* 1750 (str CO₂Ar) and 1510 cm⁻¹ (str Ar). See the synthesis section for purification information.

4-n-Decanoyloxyphenol, 6 (R=C₉H₁₉).

A soln of 22.3g (63.0 mmoles) of the ether 5 (R=C₉H₁₉) in 200 ml abs EtOH containing 1.8g of 5% Pd-C (Strem) was hydrogenated at 52° and 50 psi for 3 hr. The catalyst was removed by filtration of the rxn mixture through Celite® on hardened filter paper and the filtrate filtered again through hardened filter paper to remove traces of carbon. Removal of the solvent from the filtrate *in vacuo* gave 16.3g (98.3%) of the crude phenol with mp 68–80°. Recrystallization of

this material 3× from ligroine gave 15.0g (90.4%) of the purified phenol 6 ($R=C_9H_{19}$): mp 79–83°; TLC showed one spot with $R_f=0.11$ (R_f for 5 = 0.76) and IR ($CHCl_3$) 3400 (sharp, med OH), 3180 (br, wk OH), 1750 (str, CO_2R), 1600 (med Ar), and 1500 cm^{-1} (str Ar).

trans-1,4-Octanoylcyclohexanol, 9 ($R'=C_8H_{17}$).

A soln of 15.0g (44.1 mmole) of the benzyl ether 5 ($R'=C_8H_{17}$) in 200 ml abs EtOH containing 1.2g of 10% Pd/C (MC&B) was hydrogenated at 48° and 50 psi for 18 hr. Removal of the solvent from the filtrate *in vacuo* gave 12.3g of a colorless solid. TLC showed two spots with $R_f=0.78$ and 0.61 (R_f for 5=0.61). This material was hydrogenated again in 200 ml EtOH using 1.8g of catalyst at 72° for 5 hr and worked up in the same manner to give 17.6g of a liquid. Distillation gave 2.4g of a forerun fraction (bp up to 123°) and then 5.1g (45.1%) of the major fraction at 123–125° (8 mm) identified as the alcohol 9 ($R'=C_8H_{17}$): TLC showed one spot with $R_f=0.34$ (R_f for 5=0.53); IR (film) 3000 (wk br OH), 1700 (str CO_2R'), and no 1600 cm^{-1} absorption and NMR ($CDCl_3$, F) δ 11.72 (s, 1, OH) and 2.33–0.87 (m, 26, $C_6H_{10} + C_8H_{17}$). Calcd for $C_{15}H_{28}O_3$: C, 70.26; H, 11.00; O, 18.72. Found: C, 69.89; H, 11.16; O, 18.98.

Acknowledgments

This material is based on work partially supported by the National Science Foundation-Solid State Chemistry-Grants DMR81-15544, 83-09739, and 85-15221. We would also like to thank the Chemistry Department for the FT80 NMR spectra and for use of their EM360 NMR instrument, and Frank Herlinger who synthesized a few of the compounds studied.

References

1. M. E. Neubert, F. C. Herlinger, M. R. Jirousek and A. de Vries, *Mol. Cryst. Liq. Cryst.*, **139**, 299 (1986).
2. D. Demus, H. Demus and H. Zachke, *Flüssige Kristalle in Tabellen I* (VEB Deutscher Verlag Grundstoffindustries, Leipzig, 1974).
3. M. E. Neubert, L. T. Carlino, R. D'Sidocky and D. L. Fishel, *Liquid Crystals and Ordered Fluids*, Eds. J. F. Johnson and R. Porter (Plenum Press, New York, 1974), p. 293.
4. M. E. Neubert, R. E. Cline, M. J. Zawaski, P. Wildman and A. Ekachai, *Mol. Cryst. Liq. Cryst.*, **76**, 43 (1981).
5. M. E. Neubert, M. R. Jirousek and C. A. Hanlon, *Mol. Cryst. Liq. Cryst.*, **133**, 223 (1980).
6. M. E. Neubert, L. T. Carlino, D. L. Fishel and R. M. D'Sidocky, *Mol. Cryst. Liq. Cryst.*, **59**, 253 (1980).

7. M. E. Neubert, J. P. Ferrato and R. E. Carpenter, *Mol. Cryst. Liq. Cryst.*, **53**, 229 (1979).
8. M. E. Neubert, M. E. Stahl and R. E. Cline, *Mol. Cryst. Liq. Cryst.*, **89**, 93 (1982).
9. M. E. Neubert and A. de Vries, *Mol. Cryst. Liq. Cryst.*, in press (1987).
10. D. J. Bishop, W. O. Sprenger, R. Pindak and M. E. Neubert, *Phys. Rev. Lett.*, **49**, 1861 (1982).
11. P. A. C. Gane, A. J. Leadbetter, P. A. Tucker, G. W. Gray and A. R. Tajbakhsh, *J. Chem. Soc.*, **77**, 6215 (1982).
12. D. Demus and L. Richter, *Textures of Liquid Crystals* (Verlag Chemie, Weinheim, 1978), p. 161.
13. G. W. Gray and J. W. Goodby, *Smectic Liquid Crystals, Textures, and Structures* (Leonard Hill, London, 1984), pp. 40–41.
14. M. E. Neubert, K. Leung and W. A. Saupe, *Mol. Cryst. Liq. Cryst.*, **35**, 283 (1986).
15. D. Demus, H. J. Deutscher, D. Marzotko, H. Kresse and A. Weigeleben, *Liquid Crystals—Proceedings of an International Conference, Raman Research Institute, Bangalore*, Ed. S. Chandrasekhar (Heyden Publishers, 1980), p. 97.
16. H. Sackmann, *J. Phys.*, (Paris) **40 C3**, 5 (1979).
17. J. W. Goodby and G. W. Gray, *J. Phys.* (Paris), **40 C3**, 363 (1979).
18. R. Pindak, D. E. Moncton, S. C. Davey and J. W. Goodby, *Phys. Rev. Lett.*, **46**, 1135 (1981).
19. A. L. McClellan, *Tables of Experimental Dipole Moments* (W. H. Freeman and Co., San Francisco, 1963).
20. D. Demus and H. Zashke, *Flüssige Kristalle in Tabellen II* (VEB Deutscher Verlag für Grundstoffindustries, Leipzig, 1984).
21. J. W. Goodby, *Liquid Crystals and Ordered Fluids*, Vol. 4, Eds. A. C. Griffin and J. F. Johnson (Plenum Press, New York, 1984), p. 175.
22. W. H. de Jeu, *J. Phys.* (Paris), **38**, 1285 (1977).
23. M. Aroney, R. J. Le Fevre, R. K. Pierens and M. G. N. The, *J. Chem. Soc. (B)* 666 (1969); M. Aroney, R. J. W. Le Fevre and S. S. Chang, *J. Chem. Soc.*, 3173 (1960).
24. A. Makriyannis and J. J. Knittel, *Tet Lett.*, 2753 (1979).
25. L. A. Cohen and S. Tokahashi, *J. Am. Chem. Soc.*, **95**, 443 (1973); W. B. Schweizer and J. D. Dunitz, *Helv. Chim. Acta*, **65**, 1547 (1982).
26. J. W. Goodby, *Mol. Cryst. Liq. Cryst.*, **75**, 179 (1981).
27. A. S. Paranjpe, *Mol. Cryst. Liq. Cryst.*, **82**, 93 (1982).
28. E. Salz, J. P. Hummel, P. J. Flory and M. Plaušić, *J. Phys. Chem.*, **85**, 3211 (1981).
29. M. E. Neubert and L. J. Maurer, *Mol. Cryst. Liq. Cryst.*, **43**, 313 (1977).